

Molecular thermodynamics approach for binary polymer solutions on the non-random mixing effect

Bong Ho Chang and Young Chan Bae*

Department of Industrial Chemistry and Molecular Thermodynamics Laboratory, Hanyang University, Seoul 133-791, South Korea
(Received 18 December 1996)

The lattice model gives a starting point for a theoretical description of the thermodynamic properties of polymer solution systems. Classical models, such as the Flory–Huggins model and the quasi-chemical model, present too narrow or parabolic coexistence curves when compared with experimental data. It is well known that failures of the lattice model are due to mathematical approximations for the effects of non-random mixing in order to gain an analytical solution. Moreover, the existing configurational energy of mixing, in which the residual terms are truncated, results in significant errors in the prediction of the coexistence curve calculations for polymer solution systems.

The proposed model in this study improves the mathematical approximation defect and gives a new expression for the configurational energy of mixing. To correlate the energy of mixing term, including the effect of non-random mixing on the configurational thermodynamic properties of a binary mixture with simulation data, we use Monte-Carlo simulation data. Monte-Carlo simulation gives essentially exact results for the lattice model. The configurational Helmholtz energy is obtained upon combining the Gibbs–Helmholtz equation with Guggenheim's athermal entropy of mixing as a boundary condition. The coexistence curves generated by the proposed model are compared with experimental data. © 1997 Elsevier Science Ltd.

(Keywords: molecular thermodynamics; non-random mixing; quasi-chemical)

INTRODUCTION

Lattice models have played a frequent part in the theory of polymer solutions. A variety of polymer-solution theories have been developed during the last half-century. Molecular-based thermodynamic models for describing liquid–liquid equilibria (LLE) in polymer mixtures can be divided into four categories, each corresponding to a particular statistical mechanical framework: incompressible-lattice models, generalized van der Waals partition-function theories, compressible-lattice models^{1–3}, and off-lattice (continuous-space) models of chain fluids.

The most widely used and best known example of the incompressible-lattice model is the Flory–Huggins theory^{4–8}, which illustrates in a simple way the competition between the entropy of mixing and the attractive forces that produce liquid–liquid phase separation at low temperatures with an upper critical solution temperature. Much work has been done to improve the mathematical solution of the lattice model, including chain connectivity and non-random mixing⁹. However, the Flory–Huggins and quasi-chemical models give too narrow or parabolic liquid–liquid coexistence curves near the critical region when compared with experimental data. The previous lattice models for liquid–liquid coexistence curves show a discrepancy resulting from mathematical approximation

for considering the effect of non-random mixing. For an analytical solution to the lattice model, the Flory–Huggins model, which is only the Bragg–Williams random mixing model extended to chain systems, does not consider non-random mixing. The quasi-chemical model, which considers non-random mixing, is only accurate for small deviations from random mixing.

Furthermore, to pursue a formal 'exact' solution to the lattice model using advanced statistical-mechanical methods^{10–17}, Freed and coworkers developed a lattice field theory (or lattice cluster theory)^{10–17} for polymer/solvent systems. This theory formally provides an exact mathematical solution for the Flory–Huggins model. However, for practical reasons, the infinite series with respect to coordination number, temperature and composition in this theory are truncated at a certain order. Therefore, this theory still remains deficient for the correlation of liquid–liquid equilibria. Recently, Lambert *et al.*¹⁸ reported a new expression for $\Delta_{\text{mix}}A$ for incompressible monomer/*r*-mer mixtures obtained by correlating the Monte-Carlo simulation results. In their study, they used the algebraic form, which is a Redlich–Kister expansion¹⁹ truncated after the third term, to correlate energy of mixing data with Monte-Carlo simulation results. These improvements provide better agreement with experimental data by widening the liquid–liquid coexistence curve.

The purpose of this study is to simplify the expression of $\Delta_{\text{mix}}A$ and improve the mathematical approximation

* To whom correspondence should be addressed

defect, using the fractional form rather than the algebraic form with second-order approximation for the configurational energy of non-random mixing¹⁹. Our model is conceptually and mathematically simple. It requires only two adjustable parameters.

MODEL DEVELOPMENT

Internal and Helmholtz energies of mixing

The description of the lattice model starts with a simple cubic lattice (coordination number $Z = 6$) containing N_r sites. The lattice is filled completely by N_1 molecules of type 1, which occupy only one lattice site ($r_1 = 1$), and N_2 molecules of type 2, which occupy r_2 nearest-neighbour lattice sites (r-mer). The energy of mixing is related to the number of nearest-neighbour pairs by

$$\frac{\Delta_{\text{mix}}U}{N_r\epsilon} = \frac{1}{2} \frac{N_{12}}{N_r} \tag{1}$$

where N_{12} is the total number of 1-2 pairs and ϵ is the interchange energy.

$$\epsilon = \epsilon_{22} + \epsilon_{11} - 2\epsilon_{21} \tag{2}$$

where ϵ_{ij} is the i - j nearest-neighbour interaction energy. The Helmholtz energy of mixing ($\Delta_{\text{mix}}A$) is obtained by integrating the Gibbs-Helmholtz equation using the Guggenheim athermal entropy of mixing as boundary condition:

$$\frac{\Delta_{\text{mix}}A}{N_r kT} = \left(\frac{\Delta_{\text{mix}}A}{N_r kT} \right)_{1/\tilde{T}=0} + \int_0^{1/\tilde{T}} \frac{\Delta_{\text{mix}}U}{N_r\epsilon} d\left(\frac{1}{\tilde{T}}\right) \tag{3}$$

$$\left(\frac{\Delta_{\text{mix}}A}{N_r kT} \right)_{1/\tilde{T}=0} = \frac{\phi_1}{r_1} \ln \phi_1 + \frac{\phi_2}{r_2} \ln \phi_2 + \frac{z}{2} \times \left[\phi_1 \frac{q_1}{r_1} \ln \frac{\theta_1}{\phi_1} + \phi_2 \frac{q_2}{r_2} \ln \frac{\theta_2}{\phi_2} \right] \tag{4}$$

A dimensionless temperature is defined by $\tilde{T} = kT/\epsilon$, where T is the absolute temperature and k is Boltzmann's constant. r_i , ϕ_i and θ_i are the number of segments per molecule, volume fraction and surface fraction of component i , respectively. ϕ_i and θ_i are defined by:

$$\phi_i = \frac{N_i r_i}{N_1 r_1 + N_2 r_2} \tag{5}$$

$$\theta_i = \frac{N_i q_i}{N_1 q_1 + N_2 q_2} \tag{6}$$

where q_i is the surface area parameter;

$$zq_i = r_i(z - 2) + 2 \tag{7}$$

Correlation of simulation data

The fractional form, to improve the mathematical approximation defect and to correlate energy of mixing data from Monte-Carlo simulation¹⁸, is given by

$$\frac{2\Delta_{\text{mix}}U}{N_r\epsilon} = \phi_1\phi_2 \left[\frac{B'}{1 - A'(\phi_2 - \phi_1)} \right] \tag{8}$$

where

$$A' = a_0 + a_1 [\exp(1/\tilde{T}) - 1] \tag{9}$$

$$B' = b_0 + b_1 [\exp(1/\tilde{T}) - 1] \tag{10}$$

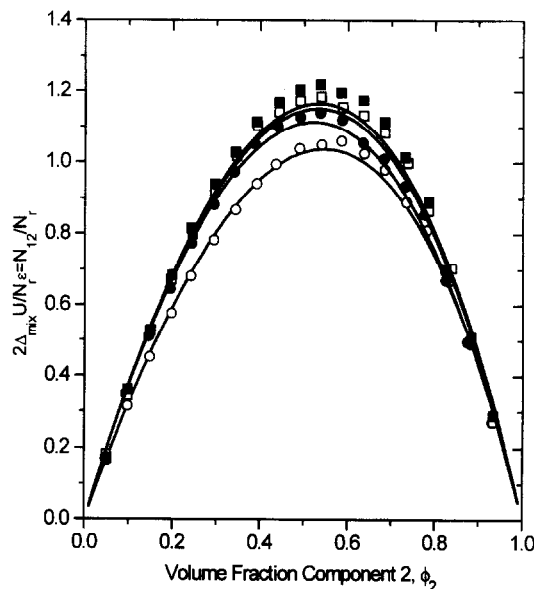


Figure 1 Plots of normalized energy of mixing for monomer (1)/20-mer (2) mixtures as a function of ϕ_2 . The open circles, solid circles, open squares and solid squares are Monte-Carlo simulation results¹⁸ for kT/ϵ values of 3, 6, 10 and ∞ , respectively. The solid lines are calculated by equation (8)

where ϕ_1 and ϕ_2 are the monomer and r-mer volume fractions, respectively. Parameters A' and B' depend on dimensionless temperature only.

Universal constants

Lambert *et al.*¹⁸ reported that a_0 , a_1 , b_0 and b_1 are very weak functions of r_2 when r_2 is adequately large. In this study, we use the same assumption. These constants are not adjustable parameters and are determined by comparison with Monte-Carlo simulation results.

Figure 1 shows the energy of mixing for monomer/20-mer mixtures as a function of r-mer volume fraction for various dimensionless temperatures. The solid lines are the fit given by equation (8) with best fitting values of a_0 , a_1 , b_0 and b_1 .

Figure 2 shows A' and B' as a function of reciprocal of dimensionless temperature. The solid lines are given by equations (9) and (10). Obtained values of a_0 , a_1 , b_0 and b_1 are 0.1057, 0.0614, 4.6846 and -1.3970 , respectively. A simple lattice model expression for predicting liquid-liquid equilibria is given by

$$\frac{\Delta_{\text{mix}}A}{N_r kT} = \left(\frac{\Delta_{\text{mix}}A}{N_r kT} \right)_{1/\tilde{T}=0} + \frac{1}{2} \phi_1\phi_2 \left[B \frac{1}{\tilde{T}} - \frac{A}{a_1(2\phi_2 - 1)} \times \ln \left\{ 1 - \frac{a_1(2\phi_2 - 1)}{1 - a_0(2\phi_2 - 1)} \{ \exp(1/\tilde{T}) - 1 \} \right\} \right] \tag{11}$$

$$A = \frac{(a_1 b_0 - a_0 b_1)(2\phi_2 - 1) + b_1}{1 + (a_1 - a_0)(2\phi_2 - 1)};$$

$$B = \frac{b_0 - b_1}{1 + (a_1 - a_0)(2\phi_2 - 1)} \tag{12}$$

and the critical condition is given by

$$\left[\frac{\partial^2 \left(\frac{\Delta_{\text{mix}}A}{N_r kT} \right)}{\partial \phi_1^2} \right]_{T,V} = \left[\frac{\partial^3 \left(\frac{\Delta_{\text{mix}}A}{N_r kT} \right)}{\partial \phi_1^3} \right]_{T,V} = 0 \tag{13}$$

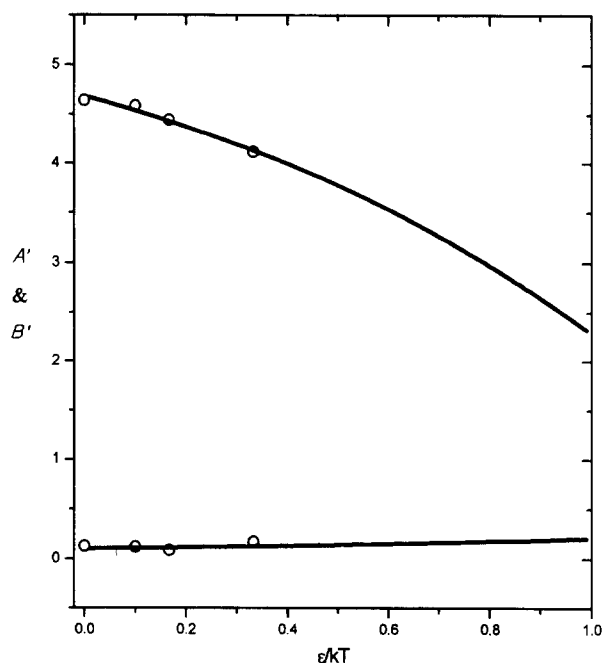


Figure 2 Plots of A' and B' as a function of reciprocal of dimensionless temperature. The upper solid line is calculated by equation (10). The lower solid line is calculated by equation (9). Open circles are values calculated by correlating with Monte-Carlo simulation results¹⁸

The critical temperature and critical volume fraction can be obtained by solving the following two equations simultaneously:

$$\begin{aligned} & \frac{-1}{1-\phi_2} + \left(1 - \frac{r_1}{r_2}\right) + \frac{Z}{2} \left[q_1 \left(\frac{\phi_2 - \theta_2}{\phi_2 \phi_1} \right) \right. \\ & \quad \left. + \left(\frac{\theta_1 \theta_2}{\phi_2 \phi_1} - 1 \right) \left(q_1 + q_2 \frac{r_1 \phi_2}{r_2 \phi_1} \right) + q_2 \frac{r_1 (\phi_1 - \theta_1)}{r_2 \phi_1^2} \right] \\ & \quad + 2r_1 \phi_2 Y 2r_1 \phi_2 (2\phi_2 - 1) \left(\frac{\partial Y}{\partial \phi_2} \right) \\ & \quad - r_1 (\phi_2^2 - \phi_2^3) \left(\frac{\partial^2 Y}{\partial \phi_2^2} \right) = 0 \end{aligned} \quad (14)$$

$$\begin{aligned} & \frac{1}{(1-\phi_2)^2} + \frac{Z}{2} \left[q_1 \frac{\{(\phi_2 \phi_1 - \theta_2 \theta_1) - (\phi_2 - \theta_2)(1 - 2\phi_2)\}}{(\phi_2 \phi_1)^2} \right. \\ & \quad \left. + \frac{\theta_1 \theta_2 (\theta_1 - \theta_2 - 1 + 2\phi_2)}{(\phi_2 \phi_1)^2} \left(q_1 + q_2 \frac{r_1 \phi_2}{r_2 \phi_1} \right) \right. \\ & \quad \left. + \left(\frac{\theta_1 \theta_2}{\phi_2 \phi_1} - 1 \right) \left(\frac{r_1 q_2}{r_2 \phi_1^2} \right) \right. \\ & \quad \left. + q \frac{r_1}{r_2} \left(\frac{\phi_2 \phi_1 + \theta_2 \theta_1 - 2\phi_2 \theta_1}{\phi_1^3 \phi_2} \right) \right] + 2r_1 Y \\ & \quad + 2r_1 (5\phi_2 - 1) \left(\frac{\partial Y}{\partial \phi_2} \right) + r_1 \phi_2 (7\phi_2 - 4) \left(\frac{\partial^2 Y}{\partial \phi_2^2} \right) \\ & \quad - r_1 (\phi_2^2 - \phi_2^3) \left(\frac{\partial^3 Y}{\partial \phi_2^3} \right) = 0 \end{aligned} \quad (15)$$

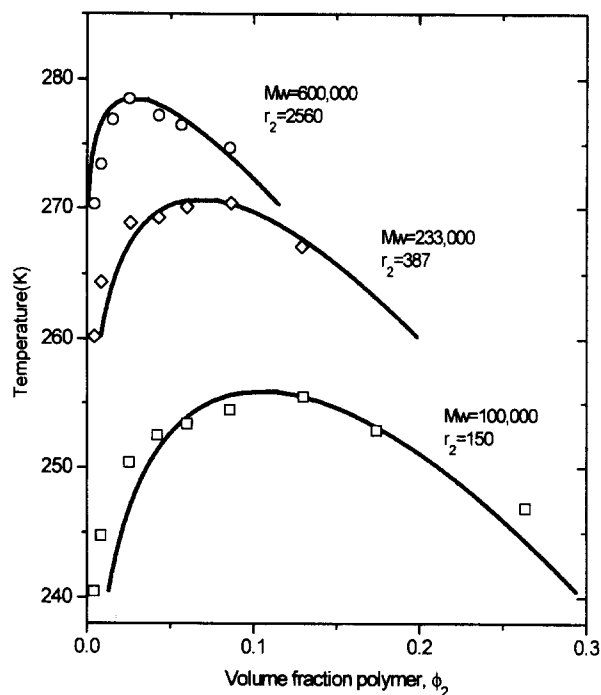


Figure 3 Coexistence curves for PS/*t*-butyl acetate systems. The open squares, diamonds and circles are experimental data²⁴ for PS molecular weights of 600 000, 233 000 and 100 000, respectively. The solid lines are calculated by equations (17) and (18)

where

$$\begin{aligned} Y = & \frac{1}{2} \left[B \frac{1}{\bar{T}} - \frac{A}{a_1 (2\phi_2 - 1)} \right. \\ & \left. \times \ln \left\{ 1 - \frac{a_1 (2\phi_2 - 1)}{1 - a_0 (2\phi_2 - 1)} \{ \exp(1/\bar{T}) - 1 \} \right\} \right] \end{aligned} \quad (16)$$

The coexistence curve is found from the conditions

$$\Delta\mu'_1 = \Delta\mu''_1 \quad (17)$$

$$\Delta\mu'_2 = \Delta\mu''_2 \quad (18)$$

where $\Delta\mu_i$ is the change in chemical potential upon isothermally transferring component i from the pure state to the mixture. Superscripts ' and '' denote two phases at equilibrium. Relative to pure component 1, the chemical potential $\Delta\mu_1$ of component 1 in the solution is defined by

$$\begin{aligned} \Delta\mu_1 = & \left(\frac{\partial \Delta_{\text{mix}} A}{\partial N_1} \right)_{T, N_2} = \ln(1 - \phi_2) + \phi_2 \left(1 - \frac{r_1}{r_2} \right) \\ & + \frac{z}{2} \left[q_1 \ln \frac{\theta_1}{\phi_1} + q_1 (\theta_2 - \phi_2) + q_2 \frac{r_1 \phi_2}{r_2 \phi_1} (\phi_1 - \theta_1) \right] \\ & + r_1 \phi_2^2 Y + r_1 \phi_2^2 \phi_1 \left(\frac{\partial Y}{\partial \phi_1} \right) \end{aligned} \quad (19)$$

and a similar relation holds for $\Delta\mu_2$

$$\begin{aligned} \Delta\mu_2 = & \left(\frac{\partial \Delta_{\text{mix}} A}{\partial N_2} \right)_{T, N_1} = \ln \phi_2 + (1 - \phi_2) \left(1 - \frac{r_2}{r_1} \right) \\ & + \frac{z}{2} \left[q_2 \ln \frac{\theta_2}{\phi_2} + q_2 (\theta_1 - \phi_2) + q_1 \frac{r_2 \phi_1}{r_1 \phi_2} (\phi_2 - \theta_2) \right] \\ & + r_2 \phi_1^2 Y + r_2 \phi_1^2 \phi_2 \left(\frac{\partial Y}{\partial \phi_2} \right) \end{aligned} \quad (20)$$

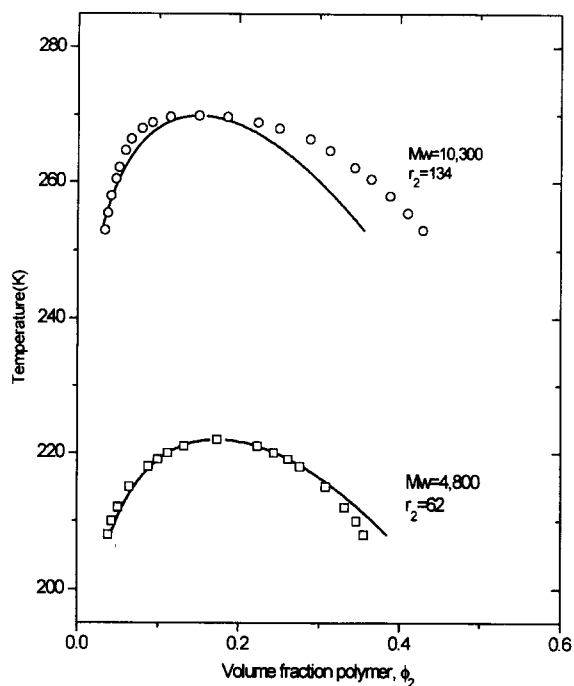


Figure 4 Coexistence curves for PS/acetone systems. The open squares and circles are experimental data²⁶ for PS molecular weights of 10 300 and 4800, respectively. The solid lines are calculated by equations (17) and (18)

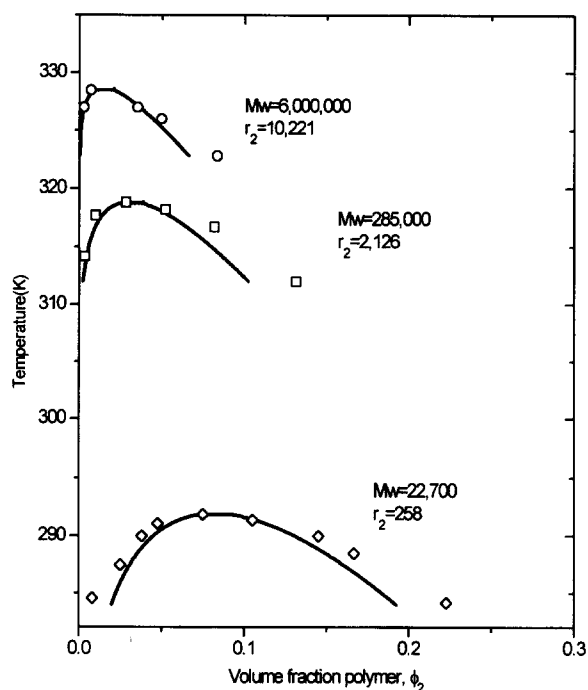


Figure 5 Coexistence curves for PIB/diisobutyl ketone systems. The open diamonds, squares and circles are experimental data²⁸ for PIB molecular weights of 6 000 000, 285 000 and 22 700, respectively. The solid lines are calculated by equations (17) and (18)

RESULTS AND DISCUSSION

It is essential to fix model parameters r_2 and ϵ/k in order to compare calculated results with experimental liquid–liquid equilibria data^{20–22}. In this study, to give agreement with the experimental results, r_2 and ϵ/k are simultaneously adjusted for all cases from equations (14)

and (15). The energy parameter, ϵ/k , has no effect on the shape of the coexistence curve. Therefore, r_2 is the most important parameter for determining the shape of the calculated coexistence curve.

Figure 3 shows phase diagrams of data for polystyrene (PS) in tert-butyl acetate^{23–26} in which only upper critical solution temperature data are compared, since specific interaction^{21,22} and free volume effect^{1–3} are not considered in the proposed model.

As shown in Figure 3, the calculated curves agree very well with experimental data. Values of ϵ/k depend weakly on the chain length of the polymer, ϵ/k values for molecular weights of 600 000, 233 000 and 100 000 are 59.6, 62.04 and 62.68 K, respectively. r_2 values are very sensitive in the calculation of coexistence curves.

Figure 4 shows phase diagrams of PS in acetone systems²⁶. ϵ/k values for PS molecular weights of 10 300 and 4800 are 72.09 and 62.21 K, respectively. A slight discrepancy shows between calculated results using the proposed model and experimental data in the high polymer concentration range. However, the model gives a reasonable prediction of critical points. For high molecular weight of polymer, there is more deviation between calculated and experimental results than those for low molecular weight of polymer. This is because the proposed model uses the simulation data for the energy of mixing for monomer/20-mer ($r_2 = 20$) mixtures.

Figure 5 shows phase diagrams of poly(isobutylene) (PIB) in diisobutyl ketone systems^{4–7}. ϵ/k values for PIB molecular weights of 6 000 000, 285 000 and 22 700 are 68.91, 68.61 and 68.59 K, respectively. In this system there are also slight deviations between calculated and experimental results. The model presented here has considered only liquid–liquid equilibria with an upper critical solution temperature, since it has not considered the oriented intermolecular forces and free volume effects which are essential for explaining lower critical solution temperatures that exist above the upper critical solution temperature²⁷.

In the proposed model, various flexibilities of chain molecules are not included. The model implicitly assumes that poly(isobutylene) (Figure 5) has the same flexibility as that of polystyrene (Figures 3 and 4). Further, solvent molecules (diisobutyl ketone in Figure 5, acetone in Figure 4, and *t*-butyl acetate in Figure 3) are considered to be monomers where the concept of flexibility does not apply. It is likely that this deficiency is basically responsible for the discrepancy between the proposed model and experimental results.

CONCLUSIONS

A simplified and improved expression of $\Delta_{\text{mix}}U$ is proposed for the Helmholtz energy of mixing for monomer/*r*-mer mixture obtained by correlating Monte-Carlo simulation results. For some binary systems, our correlating equation successfully represents liquid–liquid equilibria for various molecular weights of polymers using the same universal parameters. Our proposed model agrees well with experimental results.

ACKNOWLEDGMENT

This paper was supported by Non-Directed Research Fund, Korea Research Foundation, 1996.

REFERENCES

1. Sanchez, C. and Lacombe, R. H., *J. Phys. Chem.*, 1976, **21**, 2352, 2568.
2. Sanchez, C. and Lacombe, R. H., *Macromolecules*, 1978, **11**, 1145.
3. Sanchez, C. and Balazs, A. C., *Macromolecules*, 1989, **22**, 2325.
4. Flory, P. J., *J. Chem. Phys.*, 1942, **10**, 51.
5. Flory, P. J., *Principles of Polymer Chemistry*. Cornell University Press, Ithaca, 1953.
6. Flory, P. J., *J. Am. Chem. Soc.*, 1965, **87**, 1833.
7. Flory, P. J., *Discuss. Faraday Soc.*, 1970, **49**, 7.
8. Huggins, L., *J. Phys. Chem.*, 1942, **46**, 151.
9. Guggenheim, E. A., *Mixtures*. Clarendon Press, Oxford, Chaps. 4, 10 and 11.
10. Dudowicz, J. and Freed, K. F., *Macromolecules*, 1990, **23**, 1519.
11. Dudowicz, J. and Freed, K. F., *Macromolecules*, 1991, **24**, 5076.
12. Dudowicz, J. and Freed, K. F., *Macromolecules*, 1991, **24**, 5096.
13. Dudowicz, J. and Freed, K. F., *Macromolecules*, 1991, **24**, 5112.
14. Dudowicz, J. and Freed, K. F., *Theor. Chim. Acta*, 1992, **82**, 357.
15. Freed, K. F., *J. Phys. A: Math. Gen.*, 1985, **18**, 871.
16. Madden, W. G., Pesci, A. I. and Freed, K. F., *Macromolecules*, 1990, **23**, 1181.
17. Pesci, A. I. and Freed, K. F., *J. Chem. Phys.*, 1989, **90**, 2017.
18. Lambert, S. M., Soane, D. S. and Prausnitz, J. M., *Fluid Phase Equilibria*, 1993, **83**, 59.
19. Redlich, O., Kister, A. T. and Turnquist, C. E., *Chem. Eng. Progr. Symp. Ser. No. 2*, 1952, **48**, 49.
20. Qian, C., Mumby, S. J. and Eichinger, B. E., *Macromolecules*, 1991, **24**, 1655.
21. Hu, Y., Lambert, S. M., Soane, D. S. and Prausnitz, J. M., *Macromolecules*, 1991, **24**, 4356.
22. Hu, Y., Liu, H., Soane, D. S. and Prausnitz, J. M., *Fluid Phase Equilibria*, 1991, **67**, 65.
23. Bae, Y. C., Shim, J. J., Soane, D. S. and Prausnitz, J. M., *J. Appl. Polym. Sci.*, 1993, **47**, 1193.
24. Bae, Y. C., Lambert, S. M., Soane, D. S. and Prausnitz, J. M., *Macromolecules*, 1991, **24**, 4403.
25. Bae, Y. C., *J. Ind. & Eng. Chem.*, 1995, **1**, 18.
26. Patterson, D. and Delmas, G., *Trans. Faraday Soc.*, 1969, **65**, 708.
27. Kurata, *Thermodynamics of Polymer Solutions*. MMI Press, 1982.
28. Flory, P. J. and Schultz, 1952.